

## MOLECULAR STRUCTURE AND CONFORMATIONAL STABILITY OF COALS

Richard Sakurovs, Leo J. Lynch and Wesley A. Barton

CSIRO Division of Coal Technology, PO Box 136, North Ryde  
NSW 2113, Australia

### ABSTRACT

Factors which influence the molecular conformation and stability of the organic fractions of coals are discussed. Data for an extensive suite of Australian coals from experiments using nuclear magnetic resonance techniques to measure the effects of heating and exposure to pyridine on the stability of coal molecular structures are presented. Two types of fusible material are identified and how these materials and their fusibility vary with coal rank are evaluated. Also the rank and maceral dependence of the destabilizing effects of pyridine are catalogued.

Key Words: Coal fusibility, NMR, macerals, molecular structure.

### INTRODUCTION

#### The Molecular Properties of Coals

Dry coals are essentially organic solids at ambient temperature and, except for a degree of molecular mobility associated with aliphatic structures apparent from nuclear magnetic resonance measurements (1), they can be considered to be rigid molecular lattices. Although the molecular structures of organic substances profoundly affect their solid state properties, the molecular structure of coals has been little studied compared to their chemical composition and functionality. Studies of coal structure at any level are difficult because of the complex heterogeneity of any particular coal and the great variability of coal types that occur.

Broadly speaking three main concepts are used to model the molecular structure of coals:

- i) Coals as macromolecular three-dimensional crosslinked viscoelastic glassy solids (2,3).
- ii) Coals as macromolecular/molecular two-phase systems - the host/guest or 'rigid' and 'mobile' phase model (4-6).
- iii) Coals as paracrystalline substances depicted as having amorphous and ordered micellar regions (7).

The major limitation to the usefulness of each of these concepts (and, no doubt, the necessity for all three) stems from the great variability of coal types. Also, these concepts have mostly been applied only to the vitrinite macerals.

Conformational stability and the molecular structure of organic solids are determined both by the nature of the molecular network (how discrete molecular units are connected by covalent crosslinks) and by the nature and distribution of the various non-covalent interactions amongst these units. The non-covalent interactions include localized (e.g. hydrogen bonds) and non-localized electrostatic interactions and the short-range non-polar interactions between molecular units due to the ubiquitous and weak van der Waals induction and London dispersion forces (8).

Thus in the case of the aromatic-rich (i.e. vitrinite and inertinite) macerals of coals, if the molecular units are considered to be condensed aromatic and hydroaromatic ring structures, the molecular conformation and stability of the

macerals is determined by the density of covalent crosslinks, the degree of polar functionality and the size and geometry of the condensed ring units.

The aliphatic-rich liptinite macerals are comprised of a variety of structures including long-chain alkanes, polymerized alicyclic structures and hydroaromatic units (9). Their conformation is determined largely by covalent crosslinks and probably only to a minor extent by polar interactions.

One means of investigating molecular structures is to determine the extent to which a solid can be destabilized by heat prior to its pyrolytic decomposition.

Significant molecular mobility activated in brown coals at temperatures between 300 and 600 K has been related to the fusion of the extractable, aliphatic-rich fraction of the coals (10). Thermal destabilization of the molecular lattice of aromatic-rich macerals in bituminous coals at temperatures above ~600 K is associated with their characteristic thermoplasticity (11). The relationship between the extent of this fusion and the molecular properties of the vitrinite and inertinite macerals, however, is not well understood.

The interaction between solvents such as pyridine and coal can also be interpreted in terms of the structural features discussed above. How small nucleophilic molecules disrupt inter- and intra-molecular non-covalent interactions thereby 'relaxing' the structural matrix and allowing further solvent penetration has been extensively discussed by Peppas (12), Larsen (2,13) and Marzec (14,15) and their colleagues. Indeed the extent to which exposure to a solvent such as pyridine destabilizes a material's molecular structure is a measure of the extent to which the stability of the material depends on non-covalent and in particular polar interactions. Solvent destabilization of the molecular structure of organic materials can be quantified by simple NMR measurements at ambient temperatures. Such measurements have shown that up to ~60% of a coal's molecular structure can be destabilized by pyridine and, by the same token, that at least ~40% is impervious to pyridine (15-17).

Recently Quinga and Larsen (18) have considered the role of non-polar interactions in coals. In particular, they pointed out the likely importance of London dispersion forces between planar aromatic units and that the effect of these short-range interactions on the stability of a lattice would increase with increasing size of the molecular units. Thus the greater concentration and growth in average size of these units with increasing rank for bituminous coals lead to enhancement of the role of the London dispersion interaction in the stabilization of the molecular lattice of these coals. This process no doubt leads to the formation of the ordered graphite-like structures detectable by X-ray diffraction (e.g. ref. 7) and apparently not disrupted by exposure of the coals to pyridine and their resultant swelling (19). Also the microscopic conformal and reversible nature of the swelling of coals by pyridine established by Brenner (2) points to these ordered structures existing in microdomains of dimension less than  $\sim 10^{-6}$  m.

Strong evidence of the dominant influence of molecular structure on the properties of coals is implicit in the several data sets which show an extremum in the measured property when plotted against carbon rank. Examples are the extrema which occur in the solid state properties of mass density (20) and proton spin-lattice relaxation rate (21) as well as in solvent swelling and extractability (2).

#### Nuclear Magnetic Resonance Techniques

Proton nuclear magnetic resonance ( $^1\text{H}$  NMR) measurements can distinguish hydrogen in rigid molecular structures of coals, i.e. structures that do not undergo appreciable reorientation and/or translation during time intervals  $< \sim 10^{-5}$  s, from hydrogen in mobile structures which possess more rapid molecular motions characteristic of fused or rubbery materials. The data provided by these measurements are presented in this paper in terms of a parameter  $M_{2T}$  that measures

the extent and degree of molecular mobility.  $M_{2T}$  is an empirical second moment of the frequency spectrum of the NMR signal (22), truncated here at 16 kHz, and is inversely related to the average molecular mobility of the specimen. Thus the relative decrease in  $M_{2T}$  is a sensitive measure of the extent and degree of mobility acquired by rigid molecular structures as a result of their destabilization by thermal or solvent treatment.

The technique of  $^1\text{H}$  NMR thermal analysis yields data in the form of  $M_{2T}$  pyrograms (typical examples are shown in Figures 1 and 2). The fusibility of a coal can be ranked by the minimum value of  $M_{2T}$  ( $M_{2T}(\text{min})$ ) attained during the experiment.

Because the extensive property of a specimen measured by  $^1\text{H}$  NMR is the hydrogen content, in the data analyses described below maceral contents which are determined on a volume basis (denoted by vol%) have been converted to a wt% hydrogen basis (denoted by H-wt%) by the method of Lynch et al. (23). In practice, the changes produced in the maceral content values are small except for the coals richest in liptinite.

#### EXPERIMENTAL

Data have been obtained for an extensive suite of well characterized Australian coals by  $^1\text{H}$  NMR experiments which probe separately the effects of heat and the effects of exposure to the nucleophilic solvent pyridine on the molecular stability of the coals.

The coals and coal fractions which have been examined by  $^1\text{H}$  NMR thermal analysis are subdivided into two sets as follows:

- a) 95 Australian bituminous coals (both whole coals and maceral concentrates including 10 pairs of vitrinite and inertinite concentrates obtained by density separation) with carbon contents of 80 - 89% (daf) and hydrogen contents between 4.1 and 6% (daf);
- b) 25 sub-bituminous and brown coals with carbon contents of less than 80% (daf).

The vitrinite and inertinite (predominantly semifusinite and inertodetrinite) contents of these coals are in the ranges 10 - 98 and 5 - 80 vol% (mmf) respectively. The liptinite content never exceeds 22 vol% and is  $\leq 10$  vol% in most coals.

Pyridine swelling experiments involved a suite of 46 bituminous whole coals and maceral concentrates selected from set (a) above.

All coals were ground to  $< 500 \mu\text{m}$  and acid-washed to remove HCl-soluble iron (24). The resulting specimens were stored at 255 K under nitrogen until they were dried overnight under nitrogen at 378 K immediately prior to thermal analysis or addition of pyridine.

The thermal analysis experiments involved the collection of  $^1\text{H}$  NMR data while coal samples were being heated at 4 K/min to 875 K under non-oxidizing conditions.

In the solvent swelling study each coal was soaked in excess deuterated pyridine in a sealed glass ampoule for approximately two months before NMR measurements were made at room temperature.

#### DATA ANALYSES AND RESULTS

##### Thermal Analysis Data

In Figures 1 and 2 the  $M_{2T}$  pyrograms for seven representative coal specimens are plotted. Analytical data for these materials are listed in Table 1.

The  $M_{2T}$  pyrogram of a typical brown coal (a) reveals the significant thermally activated molecular mobility which occurs on heating from room temperature to ~ 600 K. This has been shown to be the result of fusion of the extractable component of these coals (10). The reduction in molecular mobility (increase in  $M_{2T}$ ) above 600 K results mostly from volatile loss of this 'guest' material. The  $M_{2T}$  pyrogram of the extracted residue of a brown coal (b) which constitutes usually >80% of the total coal exhibits only a low level of thermally activated molecular mobility. The shallow minimum which does occur in this pyrogram is probably due to fusion of residual 'guest' material. Thus the extract residue or 'host' component of brown coals (considered to be lignin-derived) has no significant fusion event on heating to pyrolysis temperatures at 4 K/min. This is consistent with it being a highly crosslinked macromolecular solid.

The  $M_{2T}$  pyrograms of two nominally sub-bituminous coals are recorded in Figure 1. The thermal behaviour of the lower rank Collie specimen (74.4% C) (c) is similar to that of a brown coal containing little extractable 'guest' material but its fusion is shifted to higher temperatures than that of the brown coals. The higher rank Amberley specimen (80.2% C) (d) clearly shows two fusion transitions. The first parallels that of the Collie coal until the second sharp transition occurs above 600 K. This coal has a high liptinite content (18 vol%) and a correspondingly high hydrogen content. Its high volatile matter value (47.3% daf) ranks it as a sub-bituminous coal but its carbon rank (80.2% C daf) is indicative of a lower rank bituminous coal. The second fusion transition is characteristic of lower rank thermoplastic bituminous coals but this coal has a crucible swelling number of only 2.

The high-volatile Liddell bituminous coal (Figure 2(e)) shows little indication of thermally activated molecular mobility below 500 K. There is some fusion between 500 and 600 K followed by a major fusion transition above 600 K which appears very similar to the high temperature transition of the Amberley coal. This Liddell coal, however, has only 6% liptinite, has a crucible swelling number of 6.5 and exhibits considerable Gieseler fluidity. We therefore identify this high temperature fusion event with the aromatic-rich macerals of the coal and associate it with the thermoplastic phenomenon. Hence, by implication, a stage has been reached in the coalification processes whereby aromatic-rich material becomes fusible.

The medium-volatile bituminous Bulli coal which contains no liptinite and has significant thermoplastic properties has a  $M_{2T}$  pyrogram (f) showing only one fusion transition which is lesser in extent and shifted to higher temperatures than that of the Liddell coal. This transition is, of course, attributed to aromatic-rich macerals.

The  $M_{2T}$  pyrogram for the Baralaba low-volatile semianthracite (89.7% C) (g) shows this material to be totally infusible on heating to pyrolysis temperatures.

Statistical analyses were applied to the  $M_{2T}$  data for the 120 coals in sets (a) and (b) and for those swollen with pyridine to estimate values of this parameter for 'pure average' vitrinite, inertinite and liptinite maceral groups. It was assumed that interactive effects between macerals can be neglected and hence that  $M_{2T}$  varies linearly with maceral composition, i.e.

$$M_{2T} = a * \text{vitrinite content} + b * \text{liptinite content} + c. \quad (1)$$

The regression coefficients a, b and c provide calculated  $M_{2T}$  values for 'pure' vitrinite (= 100 \* a + c), 'pure' inertinite (=c) and 'pure' liptinite (= 100 \* b + c). Because the liptinite contents span a limited range of values, extrapolations to 100% liptinite are much less reliable than those to 100% vitrinite or inertinite.

By applying this analysis at discrete 10 K temperature intervals to the NMR thermal analysis data for the 120 coals in sets (a) and (b) (subdivided into sub-bituminous and brown coals (<80% C), lower rank (80-85% C) and higher rank (85-89% C) bituminous coals), regression coefficients as functions of temperature and hence statistical  $M_{2T}$  pyrograms representative of the three maceral groups were generated (Figures 3-5). Because these pyrograms are derived statistically from data on coals with a range of thermal properties and whose petrographic specifications are subject to considerable experimental uncertainty (25), they are quantitatively imprecise and can be interpreted only in a broad qualitative manner.

The 'pure' vitrinites representative of both bituminous coal subsets remain thermally stable before the onset of fusion at temperatures above 600 K and have approximately the same maximum extent of fusion (minimum  $M_{2T}$ ) (Figures 4 and 5). The region of greatest fusion is shifted to higher temperatures for the higher rank bituminous coal subset, consistent with the expected rank dependence of coal thermoplasticity (e.g. refs. 26 and 27). (This is better demonstrated by the plot of the temperature of maximum fusion (i.e. minimum  $M_{2T}$  value) versus mean maximum vitrinite reflectance  $R_{\text{vmax}}$  for the individual coals of the set (Figure 6)).

The  $M_{2T}$  pyrograms for the 'pure' inertinites representative of the two lower rank coal subsets (Figures 3 and 4) indicate little molecular mobility in the temperature region of coal thermoplasticity (i.e.  $> 700$  K). However, the well defined minimum in the corresponding pyrogram for the higher rank bituminous coal subset reveals a degree of fusibility of inertinites in these coals.

The much greater fusibility of the liptinite macerals compared to the aromatic macerals for all ranks is clearly demonstrated by the results shown in Figures 3-5. The low temperature fusion of the sub-bituminous liptinites is similar in profile to that of the brown coal (Figure 1(a)), consistent with these liptinites containing the 'guest' materials extractable from brown and other low rank coals (28). The greater thermal stability indicated by the much higher fusion temperatures of the bituminous liptinites can be explained in terms of these materials having a more highly crosslinked macromolecular structure than the liptinites in the brown coals.

Because liptinites comprise only a small fraction of most Australian bituminous coals, their contribution to the fusibility of the whole coals is expected to be minor. Thus the  $M_{2T}$  pyrograms for typical bituminous whole coals (Figure 2(e) and (f)) closely reflect the thermal behaviour of the aromatic-rich macerals.

#### Solvent Destabilization Data

The destabilization of bituminous coal structures due to exposure to pyridine is measured by the percentage change (decrease) in the value of  $M_{2T}$  ( $\Delta M_{\text{pyr}}$ ) for the coal after two months soak. In interpreting the results for  $\Delta M_{\text{pyr}}$  we seek to isolate the separate influences of rank and maceral composition. When  $\Delta M_{\text{pyr}}$  for all the coals is plotted against vitrinite content (Figure 7), there is wide scatter and no recognizable trend. However, if the coals are separated into high (>86% C) and low (80-86% C) rank bituminous subsets (Figure 7), a strong dependence on vitrinite content for the lower rank subset becomes apparent - the greater the vitrinite content the greater the pyridine destabilization. The implication that vitrinite macerals are destabilized by pyridine to a greater extent than the other maceral types is confirmed by statistical extrapolation of the  $\Delta M_{\text{pyr}}$  values to 'pure' macerals by means of a linear regression analogous to that given by Equation 1 (results not presented here).

From Figure 7 it is also apparent that within the bituminous range the lower rank coals are destabilized by exposure to pyridine much more readily than the higher rank coals. Indeed, some higher rank specimens containing ~80 H-wt% vitrinite are little influenced by prolonged exposure (Figure 7). This rank

effect becomes clear when  $\Delta\text{Mpyr}$  is plotted against  $R_v\text{max}$  for the vitrinite-rich specimens ( $>60$  H-wt% vitrinite) (Figure 8). Above  $R_v\text{max} \sim 1.0$  the vitrinites become increasingly impervious to pyridine destabilization and it is only a minor effect when  $R_v\text{max} > \sim 1.5$ .

#### Comparison of Thermal and Pyridine Destabilization

The relationship between the extent of thermal destabilization of the molecular structures of vitrinite-rich bituminous coals on the one hand and pyridine solvent destabilization on the other is illustrated in Figure 9 in which the ratio of the decrease in  $M_{2T}$  during heating to the temperature of maximum extent of fusion to the pyridine-induced decrease  $\Delta\text{Mpyr}$  is plotted versus  $R_v\text{max}$ . For coals with  $R_v\text{max} < 1$  this ratio is independent of rank and its value of 1.5 - 2 (except for certain coals with relatively high liptinite contents which therefore enhance their overall fusibility) suggests (but does not require - see below) an appreciable commonality between the parts of the coal structure that are destabilized by solvent and by thermal treatment respectively. At higher rank the ratio tends to increase with  $R_v\text{max}$ , reflecting the reduced ability of pyridine to penetrate and destabilize molecular structures which are, however, thermally destabilized at high temperatures.

#### SUMMARY DISCUSSION

Two distinct types of fusible materials occur in coals. One type is aliphatic-rich and associated with the liptinite macerals and the other is contained in the aromatic-rich macerals and particularly the vitrinites of bituminous coals.

In the case of low rank brown coals the aliphatic-rich extractable material fuses at temperatures well below 600 K. With increasing coalification rank the thermal stability of this liptinite material increases and the temperature range of its fusion transition approaches that of the thermoplastic phenomenon of bituminous coals. The enhanced stability with increasing rank is attributed to progressive covalent crosslinking which also would make the material non-extractable. In the fused state it would remain a crosslinked 'rubbery' material resistant to solvent swelling and shear-induced flow.

Fusion in the aromatic-rich macerals is the basis of coal thermoplasticity and its occurrence in effect defines the bituminous range. Fusion within the aromatic-rich structures of low-rank sub-bituminous coals is inhibited by their high covalent crosslink density. With further coalification these crosslinks are degraded and there is loss of other functional side groups. A consequence of these processes is the consolidation of the aromatic units into microdomains or micelles (7) with increasing graphite-like order. These microdomains, stabilized by London forces, are initially small and poorly ordered. With increasing rank they become larger, more ordered and increasingly stable so that their fusion temperature rises. Thermoplasticity ceases in anthracites when these physically stabilized structures achieve a degree of stability which inhibits their fusion below their temperature of pyrolytic decomposition. This stabilization process is greatly accelerated by the rapid condensation and growth in size of the aromatic units forming the ordered domains at carbon rank  $> 87\%$  (29).

Of the aromatic-rich macerals the behaviour described above is most characteristic of the vitrinites. Inertinites are in general more oxygenated and aromatic than their corresponding vitrinites. Their much greater thermal stability and resistance to pyridine destabilization must relate to greater covalent crosslink density at all stages of coalification and this would also inhibit the development of the ordered microdomains in inertinites compared to that in the vitrinites.

# ACKNOWLEDGEMENTS

Support was provided under the National Energy Research, Development and Demonstration Program (NERDDP). T.P. Maher of the Joint Coal Board provided coal specimens and expert advice. Maceral concentrates were provided by N. Lockhart, C. Davies, M. Shibaoka, N. Ng and A. Cook. N. Thomas and Z. Lauks performed most of the thermal analysis experiments.

# REFERENCES

1. Sakurovs, R.; Lynch, L.J.; Maher, T.P.; Banerjee, R.N. *Energy Fuels* 1987, 1, 167-172.
2. Green, T.; Kovac, J.; Brenner, D.; Larsen, J.W. In 'Coal Structure'; Meyers, R.A., Ed.; Academic : New York, 1982; pp 199-282.
3. Peppas, N.A.; Lucht, L.M. *Chem. Eng. Commun.* 1984, 30, 291-310.
4. Given, P.H. In 'Coal Science'; Gorbaty, M.L., Larsen, J.W., Wender, I., Eds.; Academic : Orlando, Florida, 1984; Vol. 3, pp 63-252.
5. Marzec, A. *J. Anal. Appl. Pyrolysis* 1985, 8, 241-254.
6. Given, P.H.; Marzec, A.; Barton, W.A.; Lynch, L.J.; Gerstein, B.C. *Fuel* 1986, 65, 155-163.
7. Hirsch, P.B. *Proc. Roy. Soc. (London)* 1954, A226, 143-169.
8. Kauzmann, W. 'Quantum Chemistry'; Academic : New York, 1957; pp 503-517.
9. Neavel, R.C. In 'Chemistry of Coal Utilization'; Elliott, M.A., Ed.; 2nd Suppl. Vol.; John Wiley : New York, 1981; Chapter 3, pp 118-120.
10. Lynch, L.J.; Sakurovs, R.; Webster, D.S.; Redlich, P.J. *Fuel* 1988, 67, 1036-1041.
11. Lynch, L.J.; Webster, D.S.; Sakurovs, R.; Barton, W.A.; Maher, T.P. *Fuel* 1988, 67, 579-583.
12. For example, Peppas, N.A.; Lucht, L.M. *Chem. Eng. Commun.* 1985, 37, 333-354. Barr-Howell, B. D.; Peppas, N.A.; Winslow, D.N. *Chem. Eng. Commun.* 1986, 43, 301-315.
13. Larsen, J.W.; Green, T.K.; Kovac, J. *J. Org. Chem.* 1985, 50, 4729-4735.
14. Marzec, A.; Juzwa, M.; Betlej, K.; Sobkowiak, M. *Fuel Process. Technol.* 1979, 2, 35-44.
15. Jurkiewicz, A.; Marzec, A.; Pislewski, N. *Fuel* 1982, 61, 647-650. Marzec, A.; Jurkiewicz, A.; Pislewski, N. *Fuel* 1983, 62, 996-998.
16. Kamiński, B.; Pruski, M.; Gerstein, B.C.; Given, P.H. *Energy Fuels* 1987, 1, 45-50.
17. Barton, W.A.; Lynch, L.J. In '1987 International Conference on Coal Sciences'; Moulijn, J.A., Nater, K.A., Chermin, H.A.G., Eds.; Coal Science and Technology 11; Elsevier : Amsterdam, 1987; pp 37-40.
18. Quinga, E.M.Y.; Larsen, J.W. *Energy Fuels* 1987, 1, 300-304.

19. Bodily, D.M. The Effect of Maceral Properties on the Comminution of Coal; Final Report DOE/PC/70796-12, University of Utah, Salt Lake City, Utah, 1987. Bodily, D.M.; Wann, J-P.; Kopp, V. Prepr. Pap., Amer. Chem. Soc., Div. Fuel Chem. 1986, 31, 300-303.
20. van Krevelen, D.W. 'Coal: Typology-Chemistry-Physics-Constitution'; Coal Science and Technology 3; Elsevier : Amsterdam, 1981; Chapter 16. Thomann, H.; Silbernagel, B.G.; Jin, H.; Gebhard, L.A.; Tindall, P. Energy Fuels 1988, 2, 333-339.
21. Yokono, T.; Sanada, Y. Fuel 1978, 57, 334-336.
22. Lynch, L.J.; Webster, D.S.; Bacon, N.A.; Barton, W.A. In 'Magnetic Resonance. Introduction, Advanced Topics and Applications to Fossil Energy'; Petrakis, L., Fraissard, J.P., Eds.; NATO ASI Series C124; Reidel : Dordrecht, The Netherlands, 1984; pp 617-628.
23. Lynch, L.J.; Sakurovs, R.; Barton, W.A.; Webster, D.S.; Bacon, N.A.; Parks, T. Reactive Inertinite and Coal Carbonization -  $^1\text{H}$  NMR Thermal Analysis Studies; NERDDP End of Grant Report, Project No. 662, 1987; Chapter 5.
24. Lynch, L.J.; Sakurovs, R.; Barton, W.A. Fuel 1986, 65, 1108-1111.
25. Standard SAA AS 2856-1986. Coal - Maceral Analysis.
26. Brown, H.R.; Hesp, W.R.; Waters, P.L. J. Inst. Fuel 1964, 37, 130-139.
27. Sakurovs, R.; Lynch, L.J.; Webster, D.S.; Maher, T.P. In '1987 International Conference on Coal Science'; Moulijn, J.A., Nater, K.A., Chermin, H.A.G., Eds.; Coal Science and Technology 11; Elsevier : Amsterdam, 1987; pp 625-629.
28. Redlich, P.J.; Jackson, W.R.; Larkins, F.P. Fuel 1985, 64, 1383-1390.
29. Gerstein, B.C.; Murphy, P.D.; Ryan, L.M. In 'Coal Structure'; Meyers, R.A., Ed.; Academic : New York, 1982, pp 87-129.

TABLE 1 Analytical data for representative coals

Coal description							
	moist. (%ad)	ash(%db)	VM(%daf)	C	H	N	S
					(% daf)		
R30, Vic.	-	0.3	50.7	69.5	5.14	0.57	0.38
Collie, WA	11.9	8.1	39.4	74.4	4.31	1.32	0.91
Amberley, Qld	4.3	12.2	47.3	80.2	6.22	1.60	0.82
Liddell seam, NSW	2.8	5.8	39.5	83.4	5.63	2.19	0.41
Bulli seam, NSW	1.2	8.9	22.4	89.2	4.86	1.62	0.46
Baralaba, Qld	1.4	8.4	12.0	89.7	4.12	1.88	1.18
	R <sub>v</sub> max	Vit.	Lipt.	CSN	Gieseler		
	(%)	(%mmf)	(%mmf)		log (max fluidity, ddpm)		
R30, Vic.	-	-	-	-	-		
Collie WA	0.45	51	6	0	-		
Amberley, Qld	0.59	80	18	2	-		
Liddell seam, NSW	0.78	83	6	6.5	2.26		
Bulli Seam, NSW	1.30	46	0	7.5	1.90		
Baralaba, Qld	2.14	63	0	0.5	nd		

nd = no detectable movement

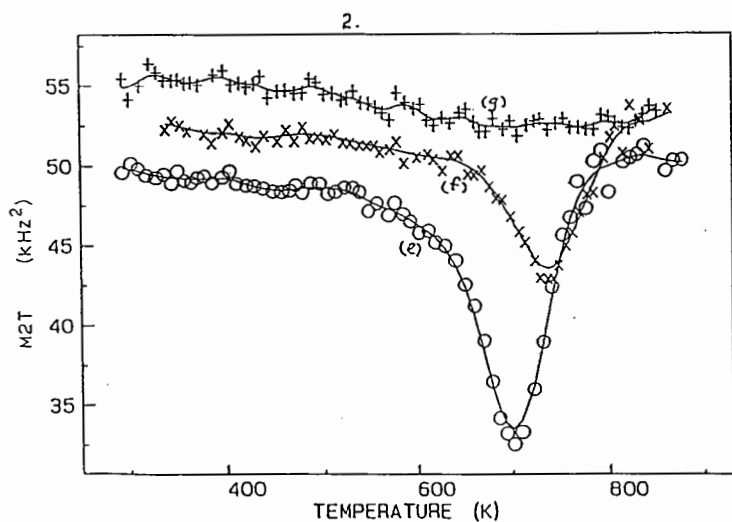
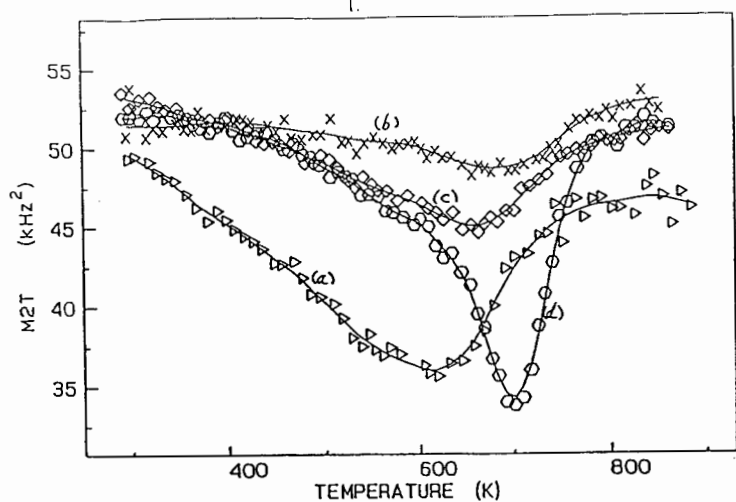


Fig. 1  $M_{2T}$  pyrograms of a brown coal (R30) (a), its extracted residue (b), and a sample of Collie (c) and Amberley (d) subbituminous coal. Analytical data in Table 1.

Fig. 2  $M_{2T}$  pyrograms of a high-volatile bituminous coal (e), a low-volatile bituminous coal (f) and a semi-anthracite (g). Analytical data in Table 1.

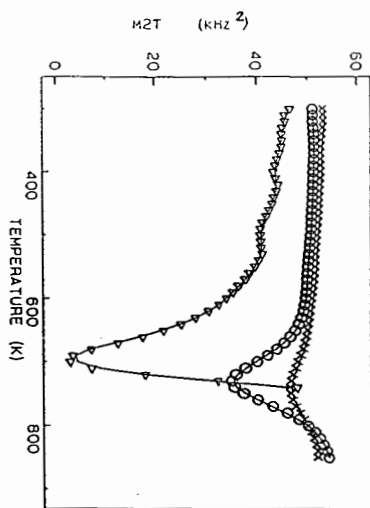


Figure 3

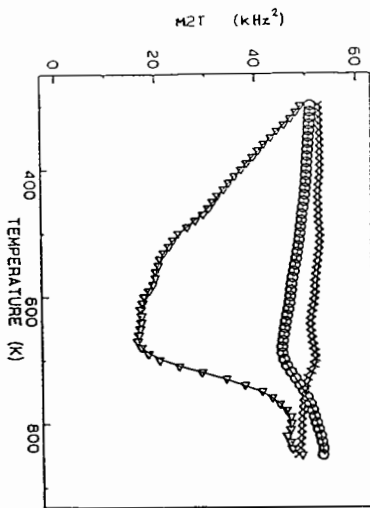


Figure 4

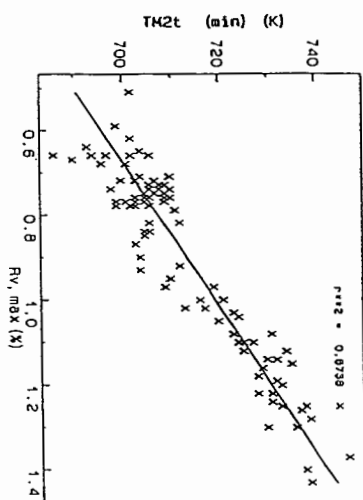


Figure 5

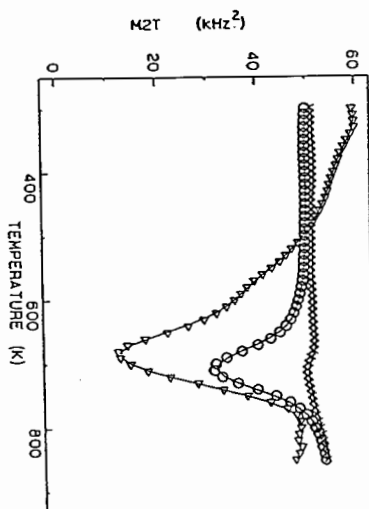


Figure 6

Fig. 3 Pyrograms of 'pure' exinite (triangles), vitrinite (o) and inertinite (x) for coals with < 80% carbon (daf).

Fig. 4 Pyrograms of 'pure' exinite (triangles), vitrinite (o) and inertinite (x) for coals with 80-85% carbon (daf).

Fig. 5 Pyrograms of 'pure' exinite (triangles), vitrinite (o) and inertinite (x) for coals with 85-89% carbon (daf).

Fig. 6 Plot of the temperature of maximum degree of fusion (TM2t(min)) against reflectance ( $R_{v,max}$ ) for bituminous coals.

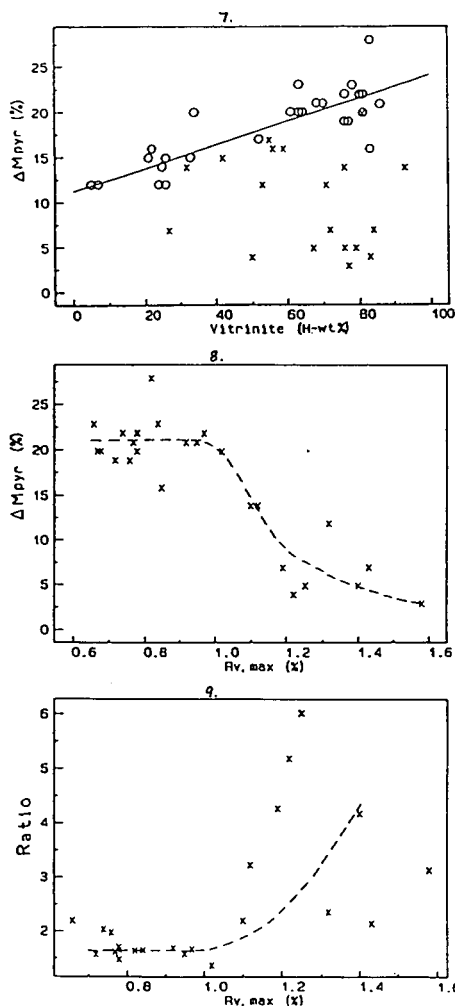


Fig. 7 Plot of  $\Delta M_{pyr}$  against vitrinite content (on a wt% hydrogen basis) for bituminous coals with 80-86% C (o) and >86% C (x). The line of best fit to these data for the lower rank subset is shown.

Fig. 8 Plot of  $\Delta M_{pyr}$  against  $R_{v, max}$  for vitrinite-rich (>60 H-wt% vitrinite) bituminous coals.

Fig. 9 Plot of the ratio of the decreases in  $M_{2T}$  due to heating and to exposure to pyridine against  $R_{v, max}$  for vitrinite-rich (> 60 H-wt% vitrinite) bituminous coals.